PHILOSOPHICAL MAGAZINE, 21 SEPTEMBER 2004
VOL. 84, NO. 27, 2829–2845

Taylor & Francis
Taylor & Francis Group

Quantized fracture mechanics

NICOLA M. PUGNO†

Department of Structural Engineering, Politecnico di Torino, Corso Duca degli Abruzzi 24, 10129, Italy

and RODNEY S. RUOFF‡

Department of Mechanical Engineering, Northwestern University, Evanston, IL 60208-3111, USA

[*Received 28 May 2004 and accepted 30 May 2004*]

ABSTRACT

A new energy-based theory, quantized fracture mechanics (QFM), is presented that modifies continuum-based fracture mechanics; stress- and strain-based QFM analogs are also proposed. The differentials in Griffith's criterion are substituted with finite differences; the implications are remarkable. Fracture of tiny systems with a given geometry and type of loading occurs at 'quantized' stresses that are well predicted by QFM: strengths predicted by QFM are compared with experimental results on carbon nanotubes, β-SiC nanorods, α-Si_3N_4 whiskers, and polysilicon thin films; and also with molecular mechanics/dynamics simulation of fracture of carbon nanotubes and graphene with cracks and holes, and statistical mechanics-based simulations on fracture of two-dimensional spring networks. QFM is self-consistent, agreeing to first-order with linear elastic fracture mechanics (LEFM), and to second-order with non-linear fracture mechanics (NLFM). For vanishing crack length QFM predicts a finite ideal strength in agreement with Orowan's prediction. In contrast to LEFM, QFM has no restrictions on treating defect size and shape. The different fracture Modes (opening I, sliding II and tearing III), and the stability of the fracture propagations, are treated in a simple way.

§ 1. INTRODUCTION

The phenomenon of fracture is of great interest. Two classic treatments are Griffith's criterion (1920), an energy-based method, and a method based on the stress-intensity factor (Westergaard 1939); these present a well-known paradox. For a linear elastic structural element containing a crack of infinitesimal length, both these methods of continuum-based linear elastic fracture mechanics (LEFM), shown to be equivalent (Irwin 1957), incorrectly predict an infinite load at failure. Conversely from elasticity, a singularity in the stress field at the crack tip (Westergaard 1939) is derived also for infinitesimal crack length; combined with the classical assumption that failure occurs when the maximum stress equals or exceeds the material strength, failure must occur at the physically unreasonable zero load. We choose to modify

† Author for correspondence. Email: n-pugno@northwestern.edu
‡ Author for correspondence. Email: r-ruoff@northwestern.edu

Philosophical Magazine ISSN 1478–6435 print/ISSN 1478–6443 online
http://www.tandf.co.uk/journals
DOI: 10.1080/14786430412331280382

fracture mechanics, by accounting for the discontinuous nature of matter at the atomic scale. By substituting the differentials in Griffith's criterion with finite differences, the paradoxes mentioned above are overcome, and a much more flexible theory, without *ad hoc* assumptions, results. We call this analytic theory quantized fracture mechanics (QFM) and show that QFM includes LEFM and NLFM as limiting cases.

QFM is particularly relevant to the fracture of tiny structures, such as of nanotubes, nanowires, and nanoplates that play, and will play, a central role in nanotechnology applications.

§ 2. Derivation of QFM

We assume a quantization of Griffith's criterion to account for discrete crack propagation, and thus in the continuum hypothesis, differentials are substituted with finite differences, i.e. $\mathrm{d}\rightarrow\Delta$. According to the principle of conservation of energy, Griffith's energy criterion implies a crack propagation when the variation of the total potential energy $\mathrm{d}W$, corresponding to a virtual increment of the crack surface $\mathrm{d}A$, becomes equal to the energy spent to create the new free crack surface, i.e., $\mathrm{d}W+G_{IC}\,\mathrm{d}A=0$, where $G_{IC}=2\gamma_{IC}$ is the fracture energy (per unit area created) of the material. The factor of 2 accounts for the creation of two surfaces during crack formation. The energy release rate is defined as $G_I=-\mathrm{d}W/\mathrm{d}A$ (where the derivation is evaluated at constant displacement), and Griffith's criterion is simply $G_I=G_{IC}$. If the fracture equilibrium state is stable the crack cannot propagate by itself (unless there were a change of loading, that is, the applied force or prescribed displacement). If the fracture equilibrium state is unstable, the crack will propagate by itself without any change of applied load or boundary displacement. The stability of the fracture equilibrium can be evaluated by the sign of the second derivative of the energy at the incipient crack propagation: if $(\mathrm{d}^2W/\mathrm{d}A^2)$ is positive, the fracture equilibrium is stable, if negative, unstable. It is well known that Griffith's criterion (1920) is equivalent to the stress-intensity factor-based criterion (Westergaard 1939) for brittle crack propagation, if the stress-intensity K_I and its critical value K_{IC} (the fracture toughness of the material) are assumed to be equal (Irwin 1957). According to LEFM (for details, see Bazant and Cedolin 1991, Hellan 1985, Carpinteri 1997), $G_I=K_I^2/E'$, with $E'=E$ (for plane stress) or $E'=E/(1-\nu^2)$ (for plane strain), where E is Young's modulus and ν is Poisson's ratio of the material. Because $G_{IC}=K_{IC}^2/E'$, the criterion $G_I=G_{IC}$ is equivalent to $K_I=K_{IC}$. Generalizing for opening (I), sliding (II), and tearing (III) crack modes, from LEFM $G=(K_I^2/E')+(K_{II}^2/E')+((1+\nu)/E)K_{III}^2$. LEFM is thus summarized as:

$$G\equiv-\mathrm{d}W/\mathrm{d}A=G_C;\ (\mathrm{d}G/\mathrm{d}A)_C<0 \text{ stable, if } >0 \text{ unstable, (LEFM)} \tag{1a}$$

$$K_{I,II,III}=K_{I,II,IIIC};\ (\mathrm{d}K_{I,II,III}^2/\mathrm{d}A)_C<0 \text{ stable, if } >0 \text{ unstable (LEFM)} \tag{1b}$$

On the other hand, in QFM ($\mathrm{d}\rightarrow\Delta$) equations (1) become:

$$G^*\equiv-\Delta W/\Delta A=G_C;\quad (\Delta G^*/\Delta A)_C<0 \text{ stable, if } >0 \text{ unstable (QFM)} \tag{2a}$$

$$K_{I,II,III}^*\equiv\sqrt{\left\langle K_{I,II,III}^2\right\rangle_A^{A+\Delta A}}=K_{I,II,IIIC};$$

$$\left(\Delta K_{I,II,III}^{*2}/\Delta A\right)_C<0 \text{ stable, if } >0 \text{ unstable (QFM)} \tag{2b}$$

where $\langle\cdot\rangle_A^{A+\Delta A} \equiv (1/\Delta A)\int_A^{A+\Delta A} \cdot \mathrm{d}A$. QFM assumes 'dissipation energy' in quanta $G_C \Delta A$ where ΔA is a *virtual* quantity that satisfies the condition that $\Delta A > 0$. Equations (1b) and (2b) are valid only for pure modes of crack propagation. For mixed modes, equations (1a) and (2a) can in principle be applied; the crack should propagate in the direction (that at nanoscale could be quantized) that maximizes the energy release rate G (LEFM; Wu 1978) or correspondingly G^* (QFM).

Values for the stress intensity factors $K_{I,II,III}$ are available (Murakami 1986) for the most interesting cases. QFM involves simply evaluating $K^*_{I,II,III}$ according to equation (2b), which also allows the stability of the process to be predicted. We thus propose QFM as a useful method for studying the strength of solids containing any shape or size defects. The hypothesis on which QFM is based is for discrete crack propagation in a linear elastic continuum medium.

2.1. *The stress analog of the energy-based QFM*

To our knowledge, only Seweryn (1998) has proposed a discrete energy release failure criterion. However, its mathematical formulation is completely different from QFM and of difficult application, since it involves the integration of the product of the complete (not only asymptotic) stress and displacement fields (which are *a priori* unknown) at the tip of the considered defect. Seweryn notes in his 'Concluding Remarks' that applying the non-local stress criterion is simpler for actual applications. The non-local stress criterion was introduced by Novozhilov (1969), who proposed a discrete fracture criterion based on stresses. He gave the condition of the brittle crack propagation in Mode I as:

$$\sigma^* \equiv \langle \sigma_y(x) \rangle_0^a = \sigma_C \tag{3a}$$

where $\sigma_y(x)$ is the complete (not only asymptotic) stress field around the defect tip ($x = 0$), σ_C is the ideal strength of the material, and a is the fracture quantum. This criterion can only be used if the complete expression of the stress-field, and not only its asymptotic term, is known; but the complete expression is rarely known. Note that this criterion could be extended for Modes II and III by replacing the normal stress with the corresponding shearing stress. Novozhilov assumed the fracture quantum to be the atomic spacing. We will show below, in the discussion of fracture strength of thin polysilicon films with self-similar holes of different sizes, the importance of relaxing this restriction by Novozhilov. For these reasons, the QFM approach of equations (2) is more powerful and at the same time, complementary to equation (3a). Novozhilov's approach, modified as stated (fracture quantum not restricted to be the atomic spacing), can be considered the stress version of QFM.

2.2. *The strain analog of the energy-based QFM*

An equivalent strain-based criterion is formulated simply by replacing the stress σ in equation (3a) with the strain ε, i.e.:

$$\varepsilon^* \equiv \langle \varepsilon_y(x) \rangle_0^a = \varepsilon_C \tag{3b}$$

The results of the discrete energy (QFM), stress- and strain-based criteria are in general expected to be close, but not identical. QFM is in general easier to apply because, as mentioned, LEFM provides the values of the stress-intensity factors for an enormous number of cases (Murakami 1986). As an example, we will compare

QFM, stress- and strain-based analogs and molecular dynamics simulations in predicting the strength of nanotubes with holes.

§ 3. Griffith's case

Consider Griffith's case of a linear elastic infinite plate in tension, of uniform thickness t, with a crack of length $2l$ orthogonal to the applied far field (crack opening Mode I). The material is described by the fracture toughness K_{IC} and by the fracture quantum at the considered size-scale $\Delta A \equiv at$. From LEFM, $K_I(l) = \sigma\sqrt{\pi l}$, where σ is the applied far field stress. According to LEFM the crack will propagate when $K_L = K_{IC}$; in contrast, for QFM the crack will propagate when

$$K_I^*(l) = \sqrt{\frac{1}{a}\int_l^{l+a} K_I^2(l)\,\mathrm{d}l} = K_{IC}.$$

The corresponding predictions for the failure strength of the plate are:

$$\sigma_{f-LEFM}(l) = \frac{K_{IC}}{\sqrt{\pi l}}, \tag{4a}$$

$$\sigma_{f-QFM}(l) = \frac{K_{IC}}{\sqrt{\pi(l + a/2)}} \tag{4b}$$

For $a/(2l) \to 0$ (i.e., large cracks) LEFM and QFM converge, whereas for $a/(2l) \to \infty$ (i.e., short cracks) they diverge. LEFM incorrectly predicts an infinite strength, whereas QFM predicts a reasonable finite strength: assuming that at the atomic scale the fracture quantum corresponds to the atomic size, the strength predicted by QFM is identical to Orowan's prediction (1948) if multiplied by a factor of $\sqrt{\pi/4}$. (Note that the prediction of QFM for vanishing crack length corresponds to the ideal strength of the material for the type of crack propagation analysed; see the Appendix). We note that equation (4b) has been previously used, but only as an empirical rule with a considered as a best fit parameter to achieve a good fit to experimental data, for predicting the behavior of short cracks for brittle fracture (Suo and Gong 1993) and fatigue (Haddad *et al.* 1980). This clearly shows that QFM also well describes the deviations from LEFM that are experimentally observed in brittle fracture and in fatigue growth of short cracks.

Note that the 'Quasi' or 'Equivalent' LEFM proposed by Irwin, which '*a priori*' considers an equivalent length of the crack (the real crack length plus the size of the 'plastic zone') is different from our approach (e.g., yields different predictions). In addition, in contrast to QFM, 'Irwin suggested (rather than provided a conclusive argument)' such an assumption (see Hellan 1985, p. 87).

For Griffith's case, brittle crack propagation is predicted to be unstable for both LEFM and QFM theories, i.e., $(\mathrm{d}K_I^2/\mathrm{d}l)_C = K_{IC}^2/l > 0$ and, $(\Delta K_I^{*2}/a)_C = K_{IC}^2/(l + a/2) > 0$.

Extending the result of equation (4b) from sharp to blunt-cracks (Creager and Paris 1967, Drory *et al.* 1995), we find an asymptotic correction (small tip radii; see Appendix) in the following form:

$$\sigma_f(l,\rho) = K_{IC}\sqrt{\frac{1 + \rho/2a}{\pi(l + a/2)}} = \sigma_C\sqrt{\frac{1 + \rho/2a}{1 + 2l/a}} \tag{5}$$

where ρ is the tip radius and $\sigma_C = \sigma_f$ ($l = 0$, $\rho = 0$). Note that if the continuum hypothesis is made (a/ρ, $a/l \to 0$), equation (5) yields practically the same result as the classical tensional approach (maximum stress equal to material strength), for which the stress concentration σ_C/σ_f is $1 + 2\sqrt{l/\rho} \approx 2\sqrt{l/\rho}$ (small radii) as given by elasticity. On the other hand, equation (5) reduces to the correct prediction of QFM for a sharp crack, equation (4b). Thus, equation (5) clarifies and quantifies in a very simple manner the link between concentration and intensification factors. The result is simple but surprising: it predicts a finite (in contrast with LEFM) strength that is size-dependent (in contrast with the continuum tensional approach coupled with elasticity) for geometrical self-similar defects in an infinite plate.

§ 4. Quantized strength levels

The fracture quantum, as suggested by equation (4b), is expected to be of the order of $2K_{IC}^2/(\pi\sigma_C^2)$, where σ_C and K_{IC} are the strength and the fracture toughness of the material at the considered size scale, respectively. For nanostructures (vanishing pre-existing defects), σ_C should be the ideal strength and the fracture quantum is expected to be close to the atomic size (distance between adjacent bonds that break during crack propagation). The length of the defects should be an integer multiple of the lattice spacing, assumed as a constant. We assume that this length is equal to the fracture quantum a, and use this assumption to make predictions for the nanoscale. Moreover, we assume defects are like blunt cracks (e.g., adjacent vacancies), so that for an n-atom defect $2l \approx na$. The final assumption is that there are negligible interactions between defect and boundary (short defect). With these hypotheses, we can apply equation (5), and the strength is expected to be quantized as:

$$\sigma_f(n) \approx \sigma_C \sqrt{1 + \frac{\rho}{2a}} (1+n)^{-1/2}, \quad n > 0 \tag{6}$$

This quantization should be experimentally detectable in nanostructures, for which a small number for n ($\approx 1-10$) should be realistic and when the number n of missing atoms is small compared with the number of atoms of the resisting cross section area adjacent to the crack (the ligament).

According to equation (6), for a linear chain of n removed atoms, $2\rho \approx a$ and the quantized strengths are, σ_C ($n = 0$, $\rho = 0$), $0.79\sigma_C$ ($n = 1$), $0.65\sigma_C$ ($n = 2$), $0.56\sigma_C$ ($n = 3$), and so on. Similar quantization is expected for different types of defects (e.g., with different values of ρ; see also section below on circular holes). This discussion shows that a forbidden band exists, such that nanostructure strengths between σ_C and $\sim 0.8\sigma_C$ should not be observed for vacancy defects. It should find use in assessing whether the ideal strength has been observed by experiment and for evaluating when n is small.

§ 5. QFM predicted strengths compared with experimental values

5.1. *β-SiC nanorods*

The theses of Sheehan (1998) and Wong (1998) report fracture bending strengths (Table 1, first row) for β-SiC nanorods oriented along the [111] direction; the maximum fracture strength, 53.4 ± 5.6 GPa was also published in (Wong *et al.* 1997), and if we assume this is the ideal strength σ_C, as suggested in the literature (Wong *et al.* 1997); note that Weixue and Tzuchiang (1999) report a calculated value of

Table 1. Clustering of experimental strength [GPa] of β-SiC nanorods, α-Si_3N_4 whiskers and MWCNTs.

β-SiC	53.4 ± 5.6	32.9 ± 3.7	$13.8 \pm 2.2, 11.6 \pm 2.9, 10.2 \pm 2.1$			
α-Si_3N_4	59	38	28	24	21	17
MWCNT	63	43	39,37,37,35,34	28,26,24,24	21,20,20,19,18,18	12,11

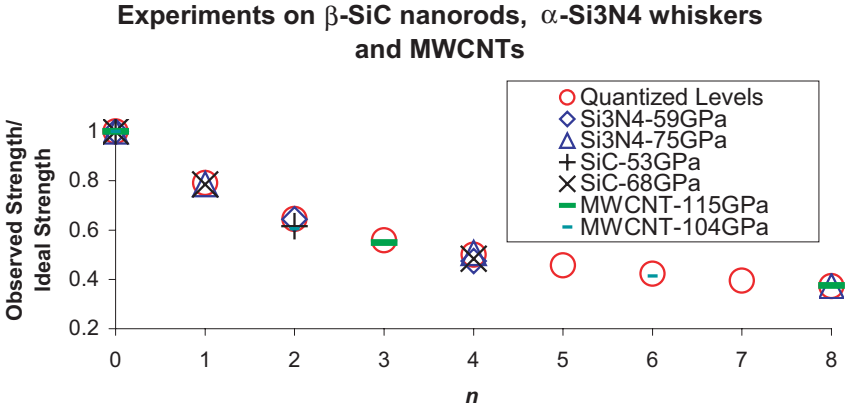

Figure 1. Quantized strength levels (observed fracture strength over ideal strength) from experiments on β-SiC nanorods, α-Si_3N_4 whiskers and MWCNTs, and QFM predicted values.

$\sigma_C = 50.8$ GPa for the [111] direction of β-SiC), QFM yields 30.8 GPa (equation (6), $n = 2$), close to the experimental value for the second highest strength measured 32.9 ± 3.7 GPa (note that equation (6) is valid also in bending, see Murakami (1986), where the failure stress is the maximum stress of the part of the nanorod in tension, and n is based on the quantized height of a small surface defect). The next value, 13.8 ± 2.2 GPa, can be interpreted by assigning $n = 4$. On the other hand, assuming 53.4 ± 5.6 GPa as $n = 1$, then 32.9 ± 3.7 GPa is best fit by $n = 4$, and the ideal strength ($n = 0$) would be $\sigma \approx 68 \pm 7.2$ GPa (we have simply multiplied the quoted error of ± 5.6 GPa by the same scaling factor of 68/53). The results are summarized in figure 1 for the two different hypotheses (β-SiC: 53 GPa $= \sigma_C$ and 68 GPa $= \sigma_C$). Fracture resulted from bending in these experiments (Wong *et al.* 1997). The probability of observing the ideal strength in bending might be greater than in pure tensile loading experiments. For bending, the volume near the clamp (where the stresses are highest) is only a small fraction of the total specimen volume.

5.2. *α-Si_3N_4 whiskers*

Experimental fracture strengths of $\alpha - Si_3N_4$ whiskers varying in diameter from 0.34 to 0.55 μm are reported by Iwanaga and Kawai (1998; Table 1, second row). Lengths were not provided in that paper (Iwanaga and Kawai 1998), but elsewhere the authors (Iwanaga and Kawai 2004, private communication) report that the typical lengths of the whiskers measured were about 1–2 mm; these $\alpha - Si_3N_4$ whiskers thus contained $\sim 10^{13}$ atoms. The observed maximum value was 59 GPa. The direction of growth for the tested whiskers was stated to be $[10\bar{1}1]$; 59 GPa can be

compared with recently calculated ideal strength values along similar (but not identical) crystal directions, which lie in the range of 51–60 GPa (Ogata *et al.* 2004); a recently calculated value for the ideal strength for loading along the $[10\bar{1}1]$ direction using identical methods to that of the previous reference, is 54 GPa (Ogata, private communication).

Assuming the highest experimental value of 59 GPa as the ideal strength; 38 GPa is well fit for $n=2$ and 28 GPa would correspond to $n=4$ (see table 1). If 59 GPa corresponds to $n=1$, the ideal strength ($n=0$) would be close to 75 GPa; 38 GPa would correspond to $n=4$, and 28 GPa to $n=8$. The results are summarized in figure 1 for the two different hypotheses (α-Si_3N_4: 59 GPa $=\sigma_C$ and 75 GPa $=\sigma_C$).

5.3. *Carbon nanotubes*

Tensile-loading experiments on the outer shell of multi-walled carbon nanotubes (MWCNTs) (Yu *et al.* 2000) show distinct clusters about a series of decreasing values of strength, with the maximum 63 GPa, and the other values 'quantized' at 43, 36–37, 25–26, 19–20 and 11–12 GPa (table 1, third row). As mentioned above, recent density functional theory (DFT) calculated values of ideal strength (Weixue and Tzuchiang 1999, Ogata *et al.* 2004) are close to the highest experimental strengths reported for β-SiC nanorods and α-Si_3N_4 whiskers. We distinguish the current dataset for experimental fracture strengths (Yu *et al.* 2000) of carbon nanotubes (CNTs) because 63 GPa is not in agreement with the ideal tensile strength of small diameter CNTs recently obtained with density functional theory. The tensile strength of an (8,8), thus armchair, CNT was calculated to be 114.6 GPa; calculated tensile strengths of 107.5, 109.0 and 107.4 GPa, respectively, were reported (Ogata and Shibutani, 2003) for three zig-zag CNTs: (8,0), (9,0) and (10,0). Another group has calculated the tensile strength of the (8,8) CNT and the (14,0) zig-zag CNT (23); these two CNTs have close to the same diameter, namely 1.09 nm (8,8) and 1.10 nm (14,0). The authors presented curves of the loading force versus tensile strain (Umeno *et al.* 2003); we used the maximum force quoted, namely 122 nN (8,8) and 128 nN (14,0); with the assumption of a 0.34-nm shell width, these correspond to tensile strengths of 104 GPa (8,8) and 110 GPa (14,0). We have simply used the two values of 115 and 104 GPa (the tensile strength values obtained by Ogata and Shibutani (2003) and Umeno *et al.* (2003) for the (8,8) CNT) as example tensile strengths of a defect-free CNT, in the analysis below. We note that the outer shell chiral angle was unknown for the 19 MWCNTs whose fracture strength was measured (Yu *et al.* 2000). With 115 (104) GPa for σ_C the measured value of 63 GPa is fit with $n=3$ ($n=2$) and the next highest experimental value of 43 GPa is fit with $n=8$ ($n=6$), as summarized in figure 1 (MWCNT 115 GPa $=\sigma_C$ and 104 GPa $=\sigma_C$). Note that these 19 outer shells, of different dimensions, were composed of between 4 and 54 million atoms. From comparison with the recent DFT and tight-binding calculations, it appears that none of the 19 MWCNTs had defect-free outer shells.

We therefore turn to comparison of QFM predicted strengths with a molecular mechanics (MM) simulation of large-diameter CNT fracture strengths where known defects were introduced, as well as comparison with molecular dynamics (MD) models of graphene sheet fracture strength as a function of an introduced crack in the side of the sheet. We also compare with a statistical mechanics treatment of fracture of one other type of two-dimensional sheet, a two-dimensional triangular lattice of springs. In these three cases one knows the defect type for treating with QFM.

§6. QFM predicted strengths compared with molecular mechanics of CNT, molecular dynamics of graphene, and statistical mechanics of 2-d spring lattices

6.1. *MM of CNT*

It has been argued that the experimental fracture strengths of the outer shell of MWCNTs (Yu *et al.* 2000) discussed above are well understood through MM analysis (Belytschko *et al.* 2002), which we here compare with QFM.

The simulations (Belytschko *et al.* 2002; MM, 0 K) on a large diameter zig-zag (80,0) CNT, which has a diameter of 6.3 nm, treated the reduction in strength due to missing pairs of carbon atoms. In the simulations, an n-atom defect was created by removing n adjacent atoms along the circumference of the nanotube; two-, four-, six- and eight-atom defects were treated. The comparison between these MM simulations and equation (6) is summarized in table 2: the MM-calculated strengths clearly follow the $(1+n)^{-1/2}$ dependence predicted by QFM. (The same quantized trend was reflected in the critical strains.) This suggests identifying the fracture quantum with the distance between two adjacent bonds, i.e., $a \approx \sqrt{3} r_0$, with $r_0 \approx 1.42$ Å, for the more likely (Appendix) 'zig-zag' fracture. The comparison using QFM, equation (6), is appropriate because of the large diameter of the experimentally investigated (Yu *et al.* 2000) and numerically modelled (Belytschko *et al.* 2002) nanotubes; the ratio between crack and circumferential lengths can be considered as negligible. We have noted the close fit to a $(1+n)^{-1/2}$ dependence; this is the fit, of course, for two-, four-, six- and eight-atom defects, with $\sigma_C \sqrt{1+\rho/2a} = 111$ GPa. For the value of the ideal strength calculated in (Belytschko *et al.* 2002), $\sigma_C = 93.5$ GPa, equation (6) gives the reasonable value of $\rho \approx 0.8a \approx 2.0$ Å.

Treating these adjacent vacancies as sharp short cracks, we can also compare our predictions with the Griffith-Inglis short crack theory, described by Weertman (1986, 1996). Details are given in the *Appendix*. The comparison is reported in table 2, showing an interesting agreement.

6.2. *MD of grapheme*

We next consider MD simulation of a cracked graphene sheet of width 9.63 nm and with four adjacent atoms missing, which resulted in a calculated failure of 52 GPa (Belytschko and Xiao 2003). By using the QFM strength values from the analysis on CNTs presented above (a relevant comparison with a graphene sheet because of the large diameter CNTs experimentally measured (Yu *et al.* 2000) and also treated by MM (Belytschko *et al.* 2002), from equation (6) we estimate $n \approx \left(\frac{111}{52}\right)^2 - 1 \approx 4$ (evaluated as 'the nearest integer') identical to the number of atoms removed in the simulation. Conversely, $\sigma_f(n=4) \approx 111/\sqrt{5} \approx 50$ GPa,

Table 2. Comparison between molecular mechanics (MM) simulations, theoretical QFM predictions (equation (6)) and Griffith–Inglis short crack theory (GI), for the strength (GPa) of nanotubes with blunt-cracks (adjacent vacancies of n atoms).

n-atom defect	2	4	6	8
MM	64.1	50.3	42.1	36.9
QFM	64.1	49.6	42.0	37.0
GI	67.9	51.7	43.3	37.9

close to 52 GPa. This example again shows that the fracture quantum is expected to be close to the 'straight line' distance between two atoms, $a = \sqrt{3}r_0$.

6.3. *Two-dimensional spring lattices*

The influence of one-, two- and three-adjacent vacancies in a two-dimensional triangular Lennard–Jones crystal was investigated by using a statistical-mechanics formulation (Selinger *et al.* 1991); the results for the strength at 0 K were 0.78, 0.69 and 0.62 of the defect-free strength, respectively. The authors noted that they expected these values to become somewhat larger with increasing temperature. By equation (6) a good fit is again given by the plausible value of $\rho \approx 0.8\,a$: 0.83, 0.69 and 0.59. In another treatment (Beale and Srolovitz 1987), that considered a two-dimensional triangular lattice with harmonic springs, the strength due to one vacancy in a two-dimensional lattice was estimated as ~0.8 the ideal strength. A reduction factor of 0.77 is again found in Hashimoto (1999) in which tight binding molecular dynamics was used to model the uniaxial tensile strength of diamond with one vacancy. Equation (6) thus represents the asymptotic behaviour in which as $n \to 0$ the ideal strength is approached, if vacancies are assumed as the defect. The detailed statistical mechanics treatment (Selinger *et al.* 1991) of the influence of defects on strength thus agrees with QFM. Note that by simply assuming $2\rho \approx a$, as in the section on quantized strength levels, the predicted strength scaling factors are, respectively, 0.79, 0.65 and 0.56 (and so on, see figure 2).

We now turn to discussing a classic problem in mechanics, that of a hole in a plate. We show that QFM can well treat recent experimental data on small circular holes in polysilicon thin films.

§ 7. Circular holes

As an example of comparison between QFM and its stress- and strain-based analogs, we derive the strength σ_f of an infinite plate with a circular hole of radius ρ, a classical problem in mechanics.

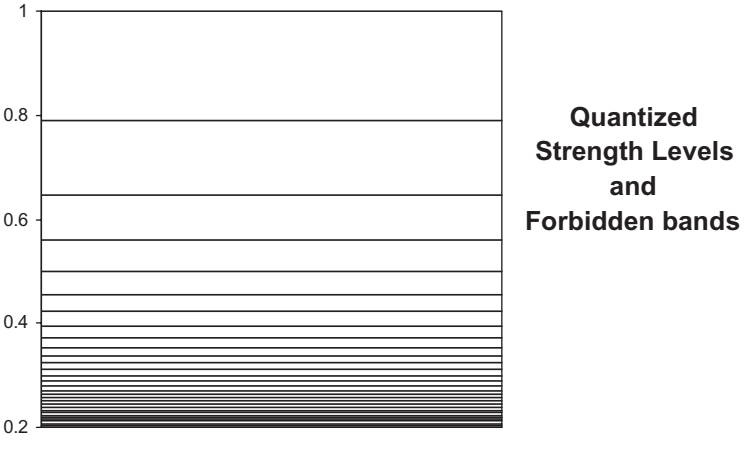

Figure 2. Example of quantized strength levels (fracture strength over ideal strength) and forbidden bands (n-atom defects, $2\rho \approx a$, equation (6)). Similar quantization is expected for different defect geometries.

QFM can be easily applied considering the expression of the stress-intensity factor at the tip of a crack emanating from a hole in a direction perpendicular to the far field stress (Tada *et al*. 1985), and then integrating according to equation (2b). On the other hand, starting from the expression of the stress-field around the hole (Kirsch 1898; see Carpinteri 1997), we find the predictions according to the strain-based QFM analog of equation (3b) (see Appendix) as:

$$\sigma_f = 2\sigma_C \Bigg/ \Bigg\{ 1 - \nu + \left(\rho^* - \rho^{*2}/(\rho^*+1)\right)(1+\nu) + \left(\left(1 - \rho^{*4}/(\rho^*+1)^3\right)(1+\nu) + 4\nu\rho^{*2}/(\rho^*+1) + \rho^* - 3\nu\rho^* \right) \cos 2\vartheta \Bigg\},$$
$$\rho^* = \frac{\rho}{a} \tag{7}$$

where ϑ is the angle describing the direction of the crack propagation with respect to the direction perpendicular to the far field. Equation (7) can be used to predict the strength of graphene sheet or 'large' nanotubes with pinhole defects. Usually $\vartheta = 0$, but for a chiral nanotube ϑ represents the chiral angle, the direction of the broken bonds (see Appendix for details) and ν is Poisson's ratio. The predictions according to the stress-based QFM analog can be obtained applying equation (3a). The result is formally equal to equation (7) in which $\nu = 0$ (here we assume plane stress and, by definition, $\varepsilon_C \equiv \sigma_C/E$, where E is Young's modulus; for plane strain $E \to E/(1-\nu^2)$, $\nu \to 1/(1-\nu)$). Below we compare QFM results with experimental results on micron-scale holes in polysilicon thin films, and also with recent MM and MD simulations of nanotubes with nanometer-scale holes.

The quantization yields the interesting result previously discussed: the strength is a function of the radius of the hole ρ and becomes equal to the classical case of $\sigma_C/3$ only by assuming the continuum hypothesis ($a/\rho \to 0$, i.e., $\rho^* \to \infty$, $\vartheta = \nu = 0$). For $\rho^* \to 0$ the hole is predicted to have no effect on the strength. Note that at small scale, we expect a minimum value for $\rho^* \sim 1/2$, which corresponds to one vacancy and to a reduction of the strength by a factor of $\sim$0.7 (this prediction is slightly different than that of 0.8 mentioned above, since they are based on different criteria).

7.1. *Experiments on polysilicon thin films with holes*

Chasiotis and Knauss (2003) present results on micro-testing experiments for different notch radii in polysilicon thin films. For circular holes of radii 1, 2, 3 and 8 μm, strength reductions, respectively, of 0.69, 0.63, 0.66, and 0.45 were measured. Noting that for polysilicon (at the considered size-scale) $\sigma_C \approx 0.85$ GPa, $K_{IC} \approx 1.5$ MPa$\sqrt{\text{m}}$ (Chasiotis and Knauss 2003), we expect $a \approx 2K_{IC}^2/(\pi\sigma_C^2) \approx 2$ μm, clearly different from the value at nanoscale. For example, with equation (7) with $\vartheta = \nu = 0$, for circular holes of radii 1, 2, 3 and 8 μm, reductions, respectively, of 0.71, 0.59, 0.53 and 0.42, are obtained. The agreement is reasonably good (although the 0.66 reduction for the 3-μm hole is off the expected trend) and shows how the classical prediction of $\sigma_C/3$ is clearly violated.

Similar experimental results are discussed in a recent paper (Bagdahn *et al*. 2003). The fracture strengths of polysilicon thin films with and without holes of radius 2.5 μm for two different film widths (20 and 50 μm) were measured; deviations from the classical value, $\sigma_C/3$, were found (note that for these finite plates, $\sigma_C/3.23$ is expected from finite element analysis for the 20-μm width, and $\sigma_C/3.04$ for the

50-μm width) (Bagdahn *et al.* 2003). In particular, we focus attention on the average values (the distribution of strengths follows a classical Weibull distribution) reported (Bagdahn *et al.* 2003), and obtain a ratio for the experimental strength of the films with and without the hole of 0.54 (20-μm width) and 0.69 (50-μm width); from equation (7) ($a \approx 2\,\mu m$, $\vartheta = \nu = 0$) we obtain 0.56.

This comparison emphasizes that at larger size scales a larger fracture quantum is expected, so that a much smaller hole would have little effect on the strength (here, a vacancy practically does not reduce the strength!); the reason is that at larger scales the materials typically have other larger defects besides the much smaller hole and such pre-existing defects are more critical than the investigated hole.

7.2. *MD simulations of carbon nanotubes with pinhole defects*

A further example is the strength of defective nanotubes with holes. Holes might be more stable than crack-like defects at the nanoscale. Nanotubes with "pinhole" defects, involving removal of 6 (defect $m = 1$) or 24 (defect $m = 2$) carbon atoms have been recently investigated in a (10,10) nanotube by MD simulation (Hirai *et al.* 2003). We estimate the radius of curvature of each hole as $\rho_m \approx (2m - 1)r_0$. Since the ratio $2\rho_m/\pi D$, with D nanotube diameter, is small (0.09 and 0.18 respectively for pinhole defects $m = 1$ and $m = 2$ in a (10,10) nanotube), we treat the nanotube as an infinite graphene sheet.

We also investigate larger values of m, where the next larger hole is generated from the previous one by removing the "next perimeter" of carbon atoms ($m = 3$, 56 atoms removed; $m = 4$, 96 atoms removed; $m = 5$, 150 atoms removed; $m = 6$, 216 atoms removed). Quantum mechanical calculations using DFT, semi-empirical quantum mechanical methods, and MM calculations, have recently been performed (Mielke *et al.* 2004) on much larger nanotubes, such as the (50, 0) and (100, 0) zig-zag tubes, with $m = 1$–6 holes (thus the ratio $2\rho_m/\pi D$ remains relatively small also for the $m = 3$, 4, 5, and 6 cases for these larger nanotubes). Applying QFM and its stress and strain analogs and using the value of $a \approx \sqrt{3}r_0$ previously deduced yields the results reported in Table 3; there is close agreement with the MM calculations on nanotubes by Mielke *et al.* (2004). Even though there is reasonable agreement for the numerically computed strength reductions of 0.80 ($m = 1$) and 0.55 ($m = 2$) for the (10, 10) nanotube by (Hirai *et al.* 2003) in our opinion these numerical results, which include

Table 3. Predicted reductions in strength of nanotubes for the presence of pinholes defects (defect $m = 1$, 6 atoms removed, $m = 2$, 24 atoms; $m = 3$, 56 atoms; $m = 4$, 96 atoms; $m = 5$, 150 atoms; $m = 6$, 216 atoms). Comparison between QFM, stress- and strain-based QFM analogs and molecular mechanics (MM) calculations on (50,0) and (100,0) zig-zag nanotubes ($\sigma_C \approx 89\,GPa$).

		QFM stress-analog (strain-analog with $\nu = 0$)	QFM strain-analog ($\nu = -0.5$)	QFM strain-analog ($\nu = +0.5$)	MM calculations on nanotubes	
σ/σ_C	QFM				(50,0)	(100,0)
$m = 1$	0.68	0.69	0.63	0.76	0.64	0.65
$m = 2$	0.48	0.51	0.47	0.55	0.51	0.53
$m = 3$	0.42	0.45	0.42	0.48	0.44	0.47
$m = 4$	0.39	0.42	0.40	0.44	0.40	0.43
$m = 5$	0.37	0.40	0.39	0.42	0.37	0.41
$m = 6$	0.36	0.39	0.38	0.40	0.34	0.39

a calculated ideal strength of ~300 GPa, do not consider an important factor. The very large computed ideal strength (as compared to the DFT calculated values of ~110 GPa (Ogata and Shibutani 2003, Umeno *et al*. 2003) suggests that there was a problem in the cut-off of the Brenner potential used (as has been discussed by Belytschko *et al*. (2002)). Thus, we consider as more relevant the comparison with the MM calculations by Mielke *et al*. (2004).

Finally, we note that in the paper by Mielke *et al*. (2004), strength reductions due to one atomic vacancy by factors of 0.81 for (10, 0) and 0.74 for (5, 5) nanotubes are close to our QFM-based prediction of 0.79.

7.3. *Experiments on carbon nanotubes*

We note that if one assumes an ideal strength of 115 GPa (as computed by DFT simulation (Ogata and Shibutani 2003) for the (8,8) nanotube) for the 20 to 40 nm diameter MWCNTs experimentally investigated (Yu *et al*. 2000) the corresponding strength (equation (7), $\vartheta = \nu = 0$) for a pinhole $m = 2$ defect is 59 GPa (measured value of 63 GPa, Table 1) and for an $m = 8$ defect is 43 GPa (measured value of 43 GPa, Table 1). This could represent another plausible scenario compared to the assumed linear defects that were previously treated by MM (Belytschko *et al*. 2002) and discussed above in Section 6.1. Indeed, Mielke *et al*. (2004) have pointed out the likelihood of large holes in the outer shells of the MWCNTs for which 19 experimental strength values (Yu *et al*. 2000) were obtained, based on the oxidation treatment used to remove extraneous carbonaceous material from the samples.

§ 8. LEFM and NLFM as limit cases of QFM

We show here that LEFM and NLFM are limit cases of QFM. In NLFM the material property G_C is replaced by an *ad hoc* resistance R (known as the R-curve) that increases, tending to G_C, by increasing the crack length. NLFM can be summarized as (for details see Hellan 1985):

$$G \equiv -\mathrm{d}W/\mathrm{d}A = R;\ (\mathrm{d}G/\mathrm{d}A)_C - (\mathrm{d}R/\mathrm{d}A)_C < 0 \text{ stable, if } > 0 \text{ unstable (NLFM)} \tag{8}$$

(Dynamic crack propagation is characterized by an excess of energy $G-R$, which is converted into kinetic energy.) Combining the conditions for crack propagation in equation (2a) and equation (8), it follows that $R = G_C + \Delta W/\Delta A - \mathrm{d}W/\mathrm{d}A$. Applying the operator $\Delta/\Delta A$ to the previous equation, it is clear that the conditions for stability in equation (2a) and equation (8) are equivalent if $\Delta G/\Delta A \equiv \mathrm{d}G/\mathrm{d}A$ and $\Delta R/\Delta A \equiv \mathrm{d}R/\mathrm{d}A$. It corresponds to a second-order expansion of W, i.e., $\Delta W \approx (\mathrm{d}W/\mathrm{d}A)\Delta A + (1/2)(\mathrm{d}^2W/\mathrm{d}A^2)(\Delta A)^2$. Consequently, equation (2a) corresponds to equation (1) (first-order approximation of QFM; QFM $\rightarrow$ LEFM), and to equation (8) (second-order approximation of QFM; QFM $\rightarrow$ NLFM), so that $R \approx G_C + (1/2) \times (\mathrm{d}^2W/\mathrm{d}A^2)_C \Delta A$. For example, applying the previous equation to the Griffith's case we find $R = G_{IC}/(1 + a/2l)$, exactly of the expected form. The classical limit of applicability of the R-curve in the NLFM treatment is that the R-curve is found as a function of the structure's geometry and not as a material property (see Bazant and Cedolin 1991); until now, it has been considered an experimental parameter. In contrast, QFM clarifies and quantifies in a very simple way the meaning of the R-curve.

§ 9. Concluding remarks

A new energy-based theory of fracture mechanics involving a modification of the well known continuum-based model has been developed that properly accounts for the discrete nature of matter (or energy release). The proposed quantized fracture mechanics (QFM) of equations (2) is self-consistent, and yields in its first-order approximation linear elastic fracture mechanics (LEFM) and in its second-order approximation non-linear fracture mechanics (NLFM). The predictions of LEFM and QFM were shown to converge for large sharp cracks, while for short cracks they diverge and only QFM correctly gives Orowan's estimate. In contrast to LEFM, which is applicable only to large sharp cracks, QFM can treat any defect shape and size. The condition for brittle crack propagation as well the stability of the process, can be evaluated for different structures, crack geometries, and modes of propagation. The application of QFM is extremely simple, allowing the prediction of the strength for any crack geometry through available stress-intensity factors that have been catalogued (Murakami 1986, Tada *et al*. 1985; i.e., an enormous number of cases). Stress- and strain-based QFM analogs have been also proposed and some examples of applications presented. Experimental results and numerical simulations for nanoscale structures agree well with QFM and its stress- and strain-based analogs.

The concept of forbidden bands for quantized strength was introduced, and should serve as a measure of whether experimental values include those close to the ideal strength.

Acknowledgements

The authors would like to thank S. Mielke, S. Zhang, D. Troya, G. Schatz, T. Belytschko, J. Achenbach, J. Weertman, B. Crist, A. Carpinteri and P. Cornetti, for many insightful discussions and A. L. Ruoff for critically reading and commenting on the manuscript prior to submission. RSR appreciates support from the NSF grant no. 0200797 ''Mechanics of Nanoropes'' (Ken Chong and Oscar Dillon, program managers), from the Office of Naval Research grant no. N00014-02-1-0870 ''Mechanics of Nanostructures'' (Mark Spector and John Pazik, program managers) and from the NASA University Research, Engineering and Technology Institute on Bio Inspired Materials (BIMat) under award No. NCC-1-02037 (Jeff Jordan, program manager).

APPENDIX A

§ A1. *Ideal strength*

Note that the prediction of QFM, for vanishing crack length, corresponds to the ideal strength of the material for the crack propagation analysed. Changing the crack propagation analysed (e.g., edge crack in a finite plate versus the Griffith's case of an (interior) crack in an infinite plate) leads to slightly different values for the 'ideal strength'. For an edge crack in a finite plate the QFM strength is 1.12 times smaller than the predicted QFM strength for the interior crack in an infinite plate (Murakami 1986). This shows that the strength, in the limiting case of vanishing defect size, cannot be considered (by QFM) separately from the analysed structure. It is plausible (certainly from an engineering perspective!) to assign the 'engineering

strength of the defect-free structure' as the smallest value resulting from analysis of the possible crack propagations leading to fracture (e.g., for a finite plate the crack would be likely to start from an edge, thus at a strength level 1.12 times smaller than as predicted by equation (4b)).

From equation (4b) the fracture quantum is expected to be of the order of $a \approx 2K_{IC}^2/(\pi\sigma_C^2)$ (neglecting the corrections, e.g., the factor 1.12 for a finite plate), where σ_C is the strength of the material (without pre-existing defects) at the considered size scale (at atomic scale, where the pre-existing defects vanish σ_C represents the ideal strength of the material). Thus the fracture quantum typically becomes larger at larger size scale. Note that the fracture quantum at larger scale sizes could be several orders of magnitude larger than the atomic size (if definable), so that a 'finite crack extension' might be a more appropriate terminology than 'fracture quantization'. (Of course, one of the goals of nanotechnology is to create defect-free materials even at large length scale.)

§ A2. *Blunt cracks*

We apply equation (3a) to predict the strength of nanostructures containing defects like chains of removed atoms, more similar to blunt-cracks (involving an atom removal, i.e., adjacent vacancies) rather than to ideal sharp nano-cracks (broken bonds, which we, and others schooled in *ab initio* calculations (Mielke *et al*. 2004), find to be less likely). Defects such as holes are also investigated (section V below).

For a blunt notch the asymptotic stress field around the tip (Creager and Paris 1967) is

$$\sigma_{asy}(x) = \frac{K_I'}{\sqrt{2\pi x}}\left(1 + \frac{\rho}{2x}\right),$$

where the origin of the reference system is in the middle between the tip and the center of the circular blunt notch, so that $x > \rho/2$, where ρ is the root notch radius and K_I' is the corresponding stress-intensity factor (the 'prime' distinguishes the case of a sharp crack). Applying equation (3a) and comparing the result with its limiting case of a sharp crack ($\rho/a = 0, K_I' = K_{IC}$) gives the asymptotic correction $K_{IC}' \approx \sqrt{1 + (\rho/2a)}\, K_{IC}$ of the critical stress-intensity factor due to the presence of the blunting (for not too large values of ρ/a, since this analysis neglects the far field with respect to the asymptotic one). As a limit case, we can consider the correction derived in (Drory *et al*. 1995) starting from the form of $\sigma_{asy}(x)$ and noting that $x > \rho/2$, i.e., $K_{IC}' \approx K_{IC}/2$.

The derived correction for the critical value of the stress-intensity factor, can be applied also for the study of nano-defects of general shape. If the profile of a defect is described by a function $y(x)$, the radius of the blunt is $\rho = (1 + (y')^2)^{3/2}/y''$, where the primes represent the derivation with respect to x (orthogonal to the applied stress). For example, for an ellipse having half-axes of length l (orthogonal to σ) and t, the radius of the blunt is $\rho = t^2/l$. In addition, since $\sigma_y(x) \approx \sigma + \sigma_{asy}(x)$, assuming an infinite plate, $K_I' = \sigma\sqrt{\pi l}$, and evaluating the stress concentration at the tip of an elliptical hole, gives $\sigma_y(x = \rho/2, K_I' = \sigma\sqrt{\pi l}, \rho = t^2/l) = \sigma(1 + 2l/t)$, thus the correct value from Elasticity.

§ A3. *Zig-zag and armchair fracture*

Even if it is clear that the fracture toughness tends to decrease with decreasing specimen size, we note that to match MM simulations (Belytschko *et al.* 2002) with equation (5), a low value of fracture toughness of $K_{IC} \approx 2\,\mathrm{MPa}\sqrt{\mathrm{m}}$ for a 'zig-zag' crack has to be assumed. A simple estimation of the fracture toughness could be obtained considering the bond dissociation energy from the Brenner potential (124 kcal/mole of C–C bonds), yielding $\gamma \approx 4.46\,\mathrm{N/m}$. Defining a 'straight line' for the edge, this value has to be multiplied by the factor $2/\sqrt{3}$ for zig-zag cracks or by the factor 4/2 for armchair cracks, so that $\gamma^{ZZ} \approx 2/\sqrt{3}\gamma$ and $\gamma^{AC} \approx 4/3\gamma$, respectively. Simply considering these values to evaluate the stress-intensity factor in Mode I as γ_{IC} (or in general $\gamma_{I,II,IIIC}$, since we expect that the fracture toughness for the different crack propagation Modes I, II and III tend to coincide at nanoscale), yields respectively $K_{IC}^{ZZ} \approx 3.21\,\mathrm{MPa}\sqrt{\mathrm{m}}$ and $K_{IC}^{AC} \approx 3.45\,\mathrm{MPa}\sqrt{\mathrm{m}}$ ($E \approx 1\,\mathrm{TPa}$).

For a zig-zag crack $a^{zz} \equiv a$, whereas for an armchair crack $a^{AC} \approx \sqrt{3}/2a^{zz}$, since the ratio of the strength corresponding to zig-zag and armchair cracks

$$\frac{\sigma^{ZZ}}{\sigma^{AC}} \approx \frac{1}{\cos\vartheta}\sqrt{\frac{\gamma^{ZZ}a^{AC}}{\gamma^{AC}a^{ZZ}}}$$

is larger than 1 for each $\vartheta < \pi/6$, zig-zag cracks are more likely than armchair cracks, as numerically observed (Belytschko *et al.* 2002) in both zig-zag and armchair, as well as chiral, nanotubes. The case of $\vartheta < \pi/6$ corresponds theoretically to $\sigma^{ZZ}/\sigma^{AC} \approx 1$, even if practically a small perturbation should lead to a 'zig-zag' crack.

Thus for a 'chiral' nanotube, we expect a zig-zag fracture, and consequently higher values of strength than for the zig-zag tubes, due to the reduction of the component of the external force acting on the bonds. Roughly, the ratio between the stress acting on the breaking bonds and the applied external stress should be close to $\cos(\vartheta)$, where ϑ is the chiral angle (note that considering the tensor nature of the stress $\cos^2(\vartheta)$ would appear instead of $\cos(\vartheta)$. Equation (7) agrees with this tensor nature of the stress, i.e., $\sigma_f(\rho = \nu = 0) = \sigma_C/\cos^2(\vartheta)$, with σ_C the strength of the bonds). The expected larger strength of chiral vs. zig-zag nanotubes agrees with MM and MD simulations (Belytschko *et al.* 2002). For example, for a zig-zag nanotube ($\vartheta = 0$) a strength of 93.5 GPa was computed, whereas for an armchair nanotube ($\vartheta = \pi/6$) 112 GPa was obtained (and for a chiral (16, 8) nanotube an intermediate value of 106 GPa was computed). The ratio 93.5/112 is equal to 0.83, between $\cos^2\pi/6 = 0.75$ and $\cos\pi/6 \approx 0.87$. Note that the same trend was numerically observed in (Ogata and Shibutani 2003).

§ A4. *Griffith–Inglis short crack theory*

According to the Griffith–Inglis short crack theory (see Weertman 1996, 1986), the prediction for the failure stress of a structure containing sharp short cracks is

$$\sigma_f = \frac{2\sigma_C}{\pi}\cos^{-1}\left(\exp\left(\frac{-\pi G\delta_C}{4(1-\nu)\sigma_C l}\right)\right),$$

where G and ν are respectively the shear elastic modulus and Poisson's ratio (that formally has to be set equal to zero for Mode III crack propagation) and δ_C is the critical tip displacement (on which the method is based). From Belytschko *et al.* (2002) $\sigma_C = 93.5\,\mathrm{GPa}$ and $E \approx 0.8\,\mathrm{TPa}$; since for nanotubes $\nu \approx 0.2$, $G \approx 0.333\,\mathrm{TPa}$. Using δ_C as a best fit parameter, we have $\delta_C \approx a/4$ (a reasonable value); the

corresponding predictions for the strength of nanotubes with short cracks of length $2l \approx 2a, 4a, 6a, 8a$ are reported in table 2 and compared with QFM and MM simulations.

§ A5. *Circular holes*

The stress near a hole of radius ρ (center at $x, y = 0$) in an infinite plate subjected to a remote stress field σ is (Kirsch 1898; see Carpinteri 1997)

$$\sigma_r = \frac{\sigma}{2}\left(1 - \frac{\rho^2}{r^2}\right) - \frac{\sigma}{2}\left(1 + 3\frac{\rho^4}{r^4} - 4\frac{\rho^2}{r^2}\right)\cos 2\vartheta,$$

$$\sigma_\vartheta = \frac{\sigma}{2}\left(1 + \frac{\rho^2}{r^2}\right) + \frac{\sigma}{2}\left(1 + 3\frac{\rho^4}{r^4}\right)\cos 2\vartheta$$

(the shearing stress does not affect our predictions). Assuming isotropic linear elastic constitutive laws and applying equation (3b) by integration, we obtain the result of equation (7), that gives the ratio between the strength σ of the element with a hole, with dimensionless radius $\rho^* = \rho/a$, and the ideal strength of the element (i.e., the strength of the element without the hole). On the other hand, applying equation (3a) we obtain the result of equation (7) if $\nu \to 0$. Assuming $\nu = \vartheta = 0$, three limit cases are interesting: (i) for $\rho^* \to 0$, $\sigma/\sigma_C \to 1$; (ii) for $\rho^* \to \infty, \sigma/\sigma_C \to 1/3$ (case of elasticity and classical tensional criterion, that assumes the continuum hypothesis, i.e., $a \to 0$); for $\rho^* \to 1/2$ (one vacancy in an ideal two-dimensional lattice), $\sigma/\sigma_C \to 0.71$.

References

Bagdahn, J., Sharpe, W. N., and Jadaan, O., 2003, *J. Microelectromech. Syst.*, **12**, 302.

Bazant, Z. P., and Cedolin, L., 1991, *Stability of Structure*: *Elastic*, *Inelastic*, *Fracture and Damage Theories* (Oxford University Press).

Beale, P. D., and Srolovitz, D. J., 1986, *Phys. Rev.* B, **37**, 5500.

Belytschko, T., and Xiao, S., 2003, *Int. J. Multiscale Comput. Engng*, **1**, 115.

Belytschko, T., Xiao, S. P., and Ruoff, R., 2002, Effects of defects on strength of nanotubes: experimental-computational comparison, *Los Alamos National Laboratory*, *Preprint Archive*, *Physics*, 1–6.

Belytschko, T., Xiao, S. P., Schatz, G. C., and Ruoff, R. S., 2003, *Phys. Rev.* B, **65**, 235430.

Blumberg Selinger, R. L., Wang, Z.-G., and Gelbart, W.M., 1991, *J. Chem. Phys.*, **95**, 9128.

Carpinteri, A., 1997, *Structural Mechanics*: *A Unified Approach* (London: Chapman & Hall).

Chasiotis, I., and Knauss, W. G., 2003, *J. Mech. Phys. Solids*, **51**, 1551.

Creager, M., and Paris, P. C., 1967, *Int. J. Fract. Mech.*, **3**, 247.

Drory, M., Dauskardt, R. H., Kant, A., and Ritchie, R. O., 1995, *J. appl. Phys.*, **78**, 3083.

El Haddad, M., Dowling, N. F., Topper, T. H., and Smith, K. N., 1980, *Int. J. Fract.*, **6**, 15.

Griffith, A. A., 1920, *Phil. Trans. Roy. Soc.*, **A221**, 163.

Hashimoto, T., 1999, *Molecular Simulation*, **23**, 143.

Hellan, K., 1985, *Introduction to Fracture Mechanics* (New York: McGraw-Hill).

Hirai, Y. *et al.*, 2003, *Jpn. J. appl. Phys.*, **42**, 4120.

Irwin, G. R., 1957, *Trans. ASME, J. appl. Mech.*, **E24**, 361.

Iwanaga, H., and Kawai, C., 1998, *J. Am. Ceram. Soc.*, **81**, 773.

Kirsch, R., July 1898, Die Theorie der Elastizitat und Die Bedurfnisse der Festigkeitslehre, *Zeitschrift Verein Duetscher Ingenieure*.

Mielke, S. L., Troya, D., Zhang, S., Li, J.-L., Xiao, S., Car, R., Ruoff, R. S., Schatz, G. C., and Belytschko, T., 2004, *Chem. Phys. Lett.*, **390**, 413.

Murakami, H., 1986, *Stress Intensity Factors Handbook* (Oxford: Pergamon).

Novozhilov, V., 1969, *Prik. Mat. Mek.*, **33**, 212.
Ogata, S., and Shibutani, Y., 2003, *Phys. Rev.* B, **68**, 165409-1/4.
Ogata, S., Hirosaki, N., Kocer, C., and Shibutani, Y., 2004, *Acta mater.*, **52**, 233.
Orowan, E., 1948, *Rep. Progr. Phys.*, **12**, 185.
Seweryn, A., 1998, *Engng. Fract. Mech.*, **59**, 737.
Sheehan, P. E., 1998, Mechanical and tribological studies at the nanometric scale, Ph.D. Thesis, *Diss. Abstr. Int., B*, **59**, 246.
Suo, Z., Ho, S., and Gong, X., 1993, *J. Engng. Mat. Tech.*, **115**, 319.
Tada, H., Paris, P. C., and Irwin, G. R., 1985, *The Stress Analysis of Cracks–Handbook*, Second Edition (Paris: Productions Incorporated).
Umeno, Y., Kitamura, T., and Matsui, E., 2003, *J. Soc. Mat. Sci. Japan*, **52**, 219.
Weertman, J., 1986, *J. appl. Phys.*, **60**, 1877; 1996, *Dislocation Based Fracture Mechanics* (Singapore: World Scientific).
Weixue, L., and Tzuchiang, W., 1999, *Phys. Rev.* B, **59**, 3993.
Westergaard, H. M., 1939, *J. appl. Mech*, **6**, 49.
Wong, E. W., 1998, Nanorods and nanotubes: synthesis, manipulation and properties, Ph.D. Thesis, *Diss. Abstr. Int. B*, **59**, 2225.
Wong, E. W., Xiao, S. P., Sheehan, P. E., Lieber, and C. M., 1997, Nanobeam mechanics: elasticity, strength and toughness of nanorods and nanotubes, *Science*, **277**, 1971.
Wu, C. H., 1978, *J. Appl. Mech.*, **45**, 553.
Yu, M.-F., Lourie, O., Dyer, M. J., Moloni, K., Kelly, T. F., and Ruoff, R. S., 2000, *Science*, **287**, 637.